ISBN: 978-3-95450-132-8 doi:10.18429/JACoW-IPAC2014-MOYBA01

THE VERY HIGH INTENSITY FUTURE*

Jie Wei#, Facility for Rare Isotope Beams, Michigan State University, MI 48824, USA

Abstract

This paper surveys the key technologies and design challenges that form a basis for the next generation of very high intensity hadron accelerators, including projects operating, under construction, and under design for science and applications at MW beam power level.

INTRODUCTION

During the past decades, accelerator-based neutron-generating facilities like SNS [1], J-PARC [2], PSI [3] and LANSCE [4] advanced the frontier of proton beam power to 1 MW level, as shown in Fig. 1 with the beam-on-target power as the product of the average beam current and the beam kinetic energy [5]. For heavy ion, the power frontier will be advanced by more than two-order-of-magnitudes to 400 kW with the construction of the Facility for Rare Isotope Beams currently underway at Michigan State University [6].

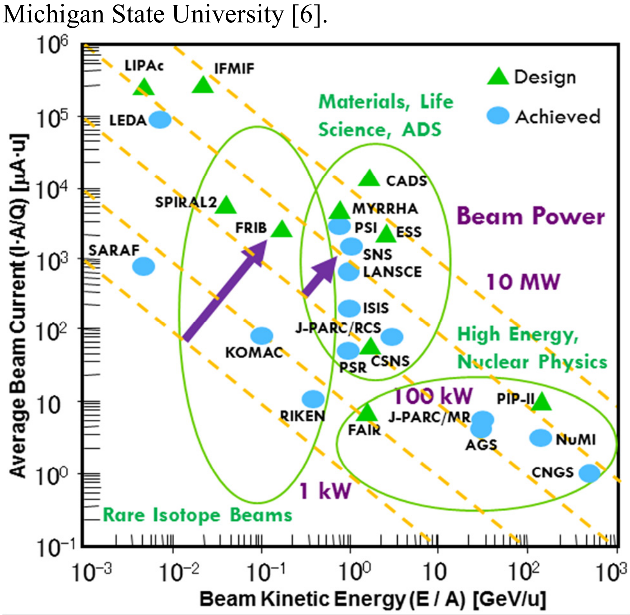

Figure 1: Hadron accelerator power frontier.

Cutting edge technologies continuously developed for accelerator systems have sustained continuous growth in beam intensity and power (Fig. 2). High-power operations have been made possible by various types of accelerators: linac, cyclotron, synchrotron and accumulator. During the past decade, superconducting RF related technology has becoming indispensable for next generation machines.

Table 1 shows some high-power hadron accelerators at design, construction, and operation stages. They are intended for high-energy physics (AGS [7], SPS [8], MI [9], J-PARC/MR [2], PIP-II [10] for neutrino, Kaon and Muon physics), nuclear physics (RIKEN [11], SPIRAL2 [12], FAIR [13], FRIB for rare isotope physics; FAIR for antiproton physics; LANSCE), basic energy science and applications (LANSCE, PSI, SNS, J-PARC/RCS [2], ISIS [14], SARAF [15], SPIRAL2, CSNS [16], ESS [17] for neutron sources; KOMAC [18] for proton applications), radioisotope production (SARAF), material neutron irradiation (IFMIF and its validation prototype LIPAc [19]), and accelerator driven subcritical systems (CADS [20] and MYRRHA [21] for nuclear waste transmutation and power generation). Other operating or proposed projects include LEDA [22], PSR [23], HIAF [24], RAON [25], CPHS [26] and those proposed at CERN (SPL, LAGUNA-LBNO, SHIP) [27] and RAL [28].

The figure of merit of these accelerator facilities is the amount of useful secondary beams produced from the target. It is proportional to the target yield and the primary beam intensity. As the optimum energy range is often determined by the target yield, high beam intensity corresponds to a high beam-on-target power.

The beam structure on target largely determines the accelerator type. Synchrotrons (AGS, SPS, MI, J-PARC, ISIS, FAIR, CSNS, PIP-II) and accumulators (PSR, SNS) are used downstream of the injector accelerators to produce pulsed beams on target. When pulsed operation is not required, cyclotrons (RIKEN and PSI) and linacs (LANSCE, KOMAC, SARAF, FRIB, SPIRAL2, IFMIF, ESS, CADS, and MYRRHA) are used to reach high beam power at high beam duty factors.

The type of primary beams is largely determined by the facility purpose. Rare isotope production using the projectile fragmentation method requires heavy ion beams (RIKEN, FRIB, SPIRAL2). Neutron production at high energy using the spallation process prefers high intensity proton beams (SNS, J-PARC, LANSCE, PSI, ISIS, CSNS, ESS, CADS, MYRRHA). Neutron production at lower energy favours deuteron beams (SARAF, IFMIF, and SPIRAL2). In synchrotron and accumulators for proton beams (ISIS, PSR, SNS, J-PARC, CSNS), the injector linac often accelerates H^- beams for multi-turn injection to reach high peak intensity on target.

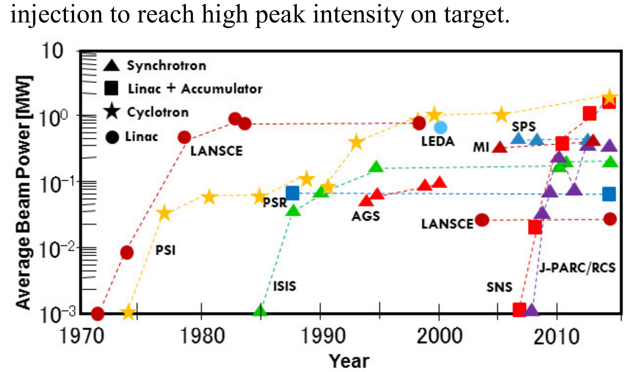

Figure 2: Achieved beam power at some major hadron facilities. Upgrade plans exist for most facilities.

*Work supported by the U.S. Department of Energy Office of Science under Cooperative Agreement DE-SC0000661
#wei@frib.msu.edu

ISBN: 978-3-95450-132-8 doi:10.18429/JACoW-IPAC2014-MOYBA01

Table 1: Major Parameters of Some Proton and Heavy Ion Accelerators at Design, Construction, and Operation Stages

Project	Status	Primary Beam	Sec. Beam	Accel. Type	f_{rep} [Hz]	Beam Duty	Target Type	Energy [MeV/u]	Ave. Power [MW]
AGS	Achieve	p	μ, K	LN/SR	0.5	5e-7;.5^{t}	Ni; Pt	24000	0.1
SPS	Achieve	p	ν	LN/SR	0.17	3.5e-6^{t}	C	400000	0.5
MI	Achieve	p	ν	LN/SR	0.75	1.e-5^{t}	C	120000	0.4
J-PARC MR	Achieve Goal	p p	ν, K, π ν, K, π	LN/SR LN/SR	0.4;0.16 1; 0.16	2e-6;.3^{t} 5e-6;.3^{t}	C; Au C; M^{r}	30000 30000	0.2; 0.02 0.75; > 0.1
LANSCE PSR	Achieve Achieve	p, H^{-} p	π, μ, n n	LN LN/AR	100 20	0.15 0.08^{i}	C^{r} W	800 800	0.8 0.08
RIKEN	Achieve Goal	d to U d to U	RIB RIB	LN/CY LN/CY	CW CW	1 1	Be Be	345-400 345-400	0.007-0.002 0.08 (U)
PSI	Achieve	p	n, μ	CY	CW	1	C^{r}, Pb	590	1.4
SNS	Achieve Goal	p p	n n	LN/AR LN/AR	60 60	0.06^{i} 0.06^{i}	Hg^{l} Hg^{l}	>940 1300	1.3 2.8
J-PARC RCS	Achieve Goal	p p	n, μ n, μ	LN/SR LN/SR	25 25	0.02^{i} 0.02^{i}	Hg^{l} Hg^{l}	3000 3000	0.3 1
ISIS	Achieve Goal	p p	n, μ n, μ	LN/SR LN/SR	40; 10 40; 10	0.01^{i} 0.01^{i}	W W	800 800	0.16; 0.04 0.45; 0.05
SARAF	Achieve Goal	p; d p, d	n; - n, RIB	LN LN	CW; 1 CW	1 1	SST;Li^{l} Li^{l}; Be	3.9; 2.8 40; 20	0.0039; - 0.2
KOMAC	Achieve	p	-	LN	10	0.005	-	100	0.01
FRIB	Constru.	p to U	RIB	LN	CW	1	C^{r}	>200	0.4
FAIR	Constru.	p to U	RIB, $\bar{p}$	LN/SR	0.2;0.5	<0.25^{i}	M^{r}; Ni	1e3;3e4	0.012;0.001
SPIRAL2	Constru.	p,d,A/q≤3	RIB, n	LN/CY	CW	1	C^{r}	33,20,14	0.2,0.2,0.04
CSNS	Constru.	p	n	LN/SR	25	0.01^{i}	W	1600	0.1
LIPAc	Constru.	d	n	LN	CW	1	Li^{l}	4.5	1.1
PIP-II	Design	p	ν, μ	LN/SR	15	0.15^{i}	C; Al	1e5; 800	1.2; 0.1
ESS	Design	p	n	LN	14	0.04	W^{r}	2000	5
IFMIF	Design	d	n	LN	CW	1	Li^{l}	20	2 x 5
CADS	Design	p	n	LN	CW	1	G+He	1500	15 – 30
MYRRHA	Design	p	n	LN	CW	1	Pb-Bi^{l}	600	1.5 – 2.4

Notation: LN for Linac; CY for Cyclotron; SR for Synchrotron; AR for Accumulator; C for graphite; M for metal; RIB for rare isotope beams; Superscripts r for rotating and l for liquid targets, i for linac beam duty and t for beam duty on target.

KEY TECHNOLOGIES

Superconducting RF (SRF)

For hadrons, SRF technology is first extensively used in the SNS linacs for the high energy-efficiency, high accelerating gradient, and operational robustness (Fig. 3) [29]. For pulsed operations, resonance control by means of fast tuners and feedforward techniques is often required to counteract Lorentz force detuning [30], and the need of higher order mode damping is to be expected [31]. FRIB as a heavy ion continuous-wave (CW) linac extends SRF to low energy of 500 keV/u. 330 low-β (from 0.041 to 0.53) cavities are housed in 49 cryomodules. The resonators (at 2 K temperature) and magnets (at 4.5 K) supported from the bottom to facilitate alignment and the cryogenic headers suspended from the top for vibration isolation. High performance subsystems including resonator, coupler, tuner, mechanical damper, solenoid and magnetic shielding are necessary [32].

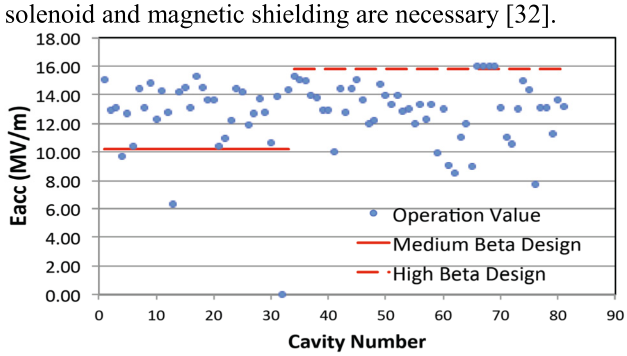

Figure 3: Accelerating gradients of the 81 SNS β=0.61 (medium) and β=0.81 (high) cavities in 23 cryomodules.

ISBN: 978-3-95450-132-8 doi:10.18429/JACoW-IPAC2014-MOYBA01

Large-scale Cryogenics

An integrated design of the cryogenic refrigeration, distribution, and cryomodule systems is key to efficient SRF operations. The FRIB refrigeration system adopts the floating pressure process – Ganni Cycle [33] for efficient adaptation to the actual loads. Distribution lines are segmented and cryomodules are connected with the U-tubes to facilitate stage-wise commissioning and maintenance (Fig. 4). The 4-2 K heat exchangers are housed inside the cryomodules for enhanced efficiency.

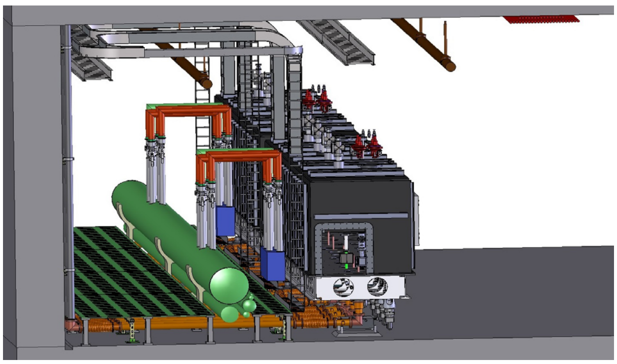

Figure 4: FRIB cryomodule with U-tube connections.

Loss Detection and Machine Protection

Machine protection is crucial to the availability of the high power accelerators. FRIB adopts multi-time scale, multi-layer approaches: the fast protection system (FPS) is designed to prevent damage from acute beam loss by quickly activating the beam inhibit device; the run permit system (RPS) continuously queries the machine state and provides permission to operate with beam; the even slower but highly sensitive RPS prevent slow degradation of SRF system under small beam loss (Table 2).

Table 2: Machine Protection for the FRIB Driver Linac

Mode	Time	Detection	Mitigation
FPS	~ 35 μs	LLRF controller; Dipole current monitor; Differential BCM; Ion chamber monitor; Halo monitor ring; Fast neutron detector; Differential BPM	LEBT bend electro-static deflector
RPS (1)	~ 100 ms	Vacuum status; Cryomodule status; Non-dipole PS; Quench signal	As above; ECR source HV
RPS (2)	> 1 s	Thermo-sensor; Cryo. heater power	As above

Challenges remain for intense low-energy heavy ion beams due to the low detection sensitivity and high power concentration/short range. Innovative techniques include the halo monitor ring [34] for high-sensitivity loss detection and current monitoring modules for critical magnet power supply inhibition. ADS machines like MYRRHA demand mean-time-between-failure of trips exceeding 3 s to be longer than 250 h [19].

Front End (Ion Source, RFQ, LEBT Transport)

Among a wide range of ion sources meeting different primary-beam requirements, ECR sources are essentially the only choice for high intensity (CW), high charge state beams. ECRs continue to move to higher RF frequency and magnetic field. High power ECR sources operate at frequencies up to 28 GHz and RF power of ~15 kW [35]. The required SC sextupole and solenoid push the state-of-the-art in SC technology. Cesium-seeded, volume production sources are most promising for the demand on high current, long pulse, low emittance H^- beams [36].

Four-vane, room temperature RFQs are commonly used for high intensity operations. LEDA RFQ with a variable voltage profile accelerated 100 mA CW proton beam to 6.7 MeV [37]. Alternatively, RFQ with trapezoidal vane modulation is tested for shunt impedance and acceleration efficiency enhancement [38]. The LEBT transport between the source and RFQ is often used for chopping, collimation, beam inhibition, and prebunching.

High-power Charge Stripping

Intense heavy ions at low energies may cause severe damage on stripping material. Innovative stripping mechanisms are under development worldwide. RIKEN uses helium gas with differential pumping (Fig. 5) [39]. Plasma windows are being tested to establish a high gas density [40]. FRIB uses a liquid lithium film moving at ~50 m/s speed. Tests with a proton beam produced by the LEDA source demonstrated that power depositions similar to the FRIB uranium beams could be achieved without destroying the film (Fig. 6) [41].

Injection of intense H^- beams into rings require sophisticated charge stripping designs [5]. Innovative schemes like laser stripping are tested [42]. Stripping can also be used to split H^- beam to multiple beam lines [43].

Figure 5: Test of He gas charge stripper using Uranium beams at RIKEN [39].

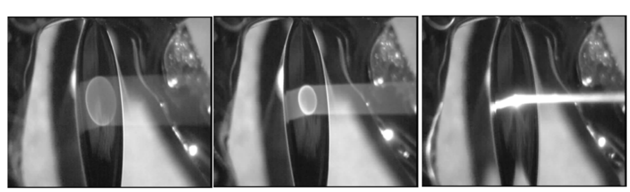

Figure 6: Liquid lithium film intercepting a proton beam of ~ 60 kV for beam power survival test [41].

ISBN: 978-3-95450-132-8 doi:10.18429/JACoW-IPAC2014-MOYBA01

Collimator

Collimators are indispensable to reduce uncontrolled beam loss for hands-on maintainability [5]. Collimation can be performed in both the transverse and longitudinal phase space (momentum cleaning and beam gap cleaning). Charge stripping is often used for H^- and partially stripped heavy ions for efficient collimation. Multi-stage collimations are used on fully stripped beams like protons [44] (Fig. 7).

For heavy ions, beams of unwanted charge states need to be removed downstream of the stripper. Such "charge selector" must sustain high power, low energy beams of short range. The FRIB charge selector, designed to absorb ~42 kW of heavy ions at 12 – 20 MeV/u, consists of two rotating graphite discs similar to the FRIB target [45].

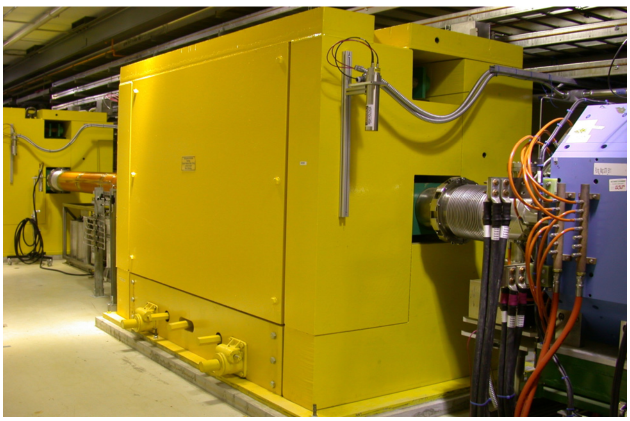

Figure 7: SNS two-stage, multi-layered collimators, each designed to withstand 10 kW protons at 1 GeV.

Target, Radiation-resistant Magnets, Handling

Target scenario is chosen based on secondary-beam requirements [46]. High-power primary beams often demand non-stationary targets like circulating liquid or rotating solid targets. For pulsed neutron production at MW level, both SNS and J-PARC/RCS use liquid mercury. Target pitting issues are largely mitigated by vessel surface treatment, mercury flow and bubble controls [47]. For lower-energy neutron production both SARAF [48] and IFMIF use liquid lithium (Fig. 8) while SPIRAL2 prefers a rotating carbon wheel. MYRRHA's ADS target uses liquid Pb-Bi eutectic [49]. For in-flight RIB production FRIB needs to focus 400 kW of heavy ion beam onto an area of 1 mm diameter (~60 MW/cm^3). A radiation-cooled multi-slice graphite target of 30 cm diameter rotates at 5000 rpm [45]. While neutron targets are designed to absorb most beam power, FRIB's RIB target is designed to absorb ~25% power; targets for high-energy physics (ν, μ, K) typically absorb <5% power.

Radiation resistance is important for magnets in the target region. Quadrupoles wound with mineral-insulated cables are built as an integral part of the shielding in front of the SNS target [50]. Quick-disconnect vacuum flanges and remote water fittings allow easy access. FRIB uses high-temperature SC magnets (YBCO) in the high radiation area of the target and primary beam dump [51].

Rapid-cycling Synchrotron Technology

At the AGS Booster, resonance corrections of magnetic nonlinearities are essential during high-intensity operations [52]. Back-leg winding driven sextupole correctors allowed for metal vacuum chambers in rapid cycling synchrotrons avoiding ceramic chamber complications [53]. ISIS uses dynamic tune variation to mitigate space charge, chromaticity, instability and coupling issues [54]. Successfully hardware systems include collimators and ceramic vacuum chambers with supported internal stainless-steel wires, interrupted with ceramic-chip capacitors to allow the passage only of beam image charge at high frequency [55].

J-PARC [2,56] advanced technologies pioneered by AGS [7] and ISIS [14] for rapid-cycling synchrotrons including introducing main magnets built with braided aluminium coil, high-gradient wideband RF cavity built with water-cooled magnetic alloy, and large aperture ceramic vacuum chamber with RF shielding (Fig.9). A large beam chamber aperture and accurate magnet tracking limit the uncontrolled beam loss below 1%.

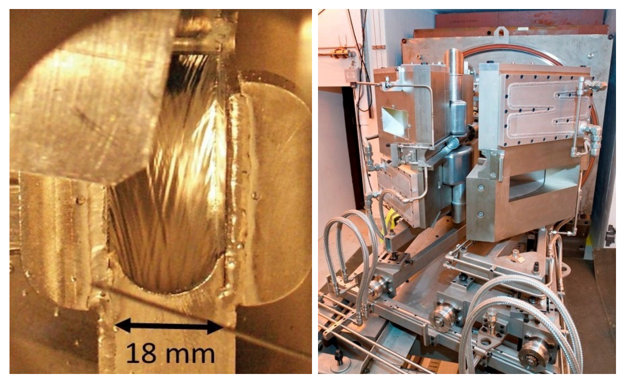

Figure 8: (left) SARAF's liquid lithium target under test [48] and ISIS spallation target station 2 [46].

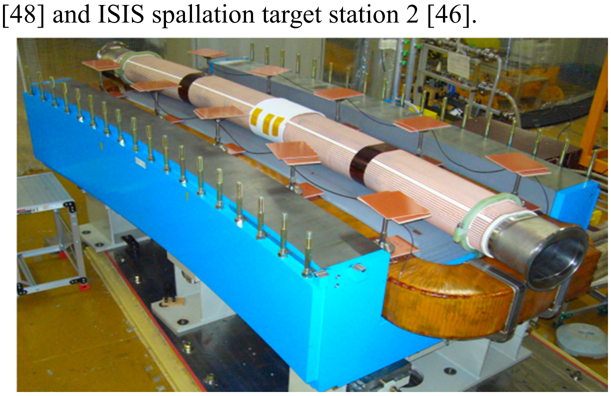

Figure 9: J-PARC RCS dipole and vacuum chamber.

Site-specific Challenges

FRIB is sited in the middle of university campus with tight real estate constraints. The driver linac is "folded" twice demanding special design considerations. The folding segments must be designed as 2nd order achromats allowing a wide momentum acceptance. Beam loss at high energy interferes with loss detection of low-energy beams. Hazard analysis upon beam faults is complicated, and installation and commissioning are interlaced.

ISBN: 978-3-95450-132-8 doi:10.18429/JACoW-IPAC2014-MOYBA01

Finally, as the linac service/utility area and cryogenics area are near the accelerator tunnel housing cryomodules, the vibration issue must be carefully addressed.

ACCELERATOR PHYSICS CHALLENGES

Examples of accelerator design challenges for high power accelerators are discussed below.

Beam Loss Control

Key to the design and operations of a high-power accelerator is to control the beam loss. Measures of loss control include beam collimation, beam dump and shielding for charge stripping and charge selection (Table 3). Uncontrolled losses must be kept below a level (about 1 W/m for protons around 1 GeV and less stringent for heavy ions [57]) to facilitate hands-on maintenance. Personnel protection system is designed against radiation exposure under both normal and fault machine conditions.

Table 3: Estimated FRIB beam losses

Type and location	Energy [MeV/u]	Peak power	Duty factor
Uncontrolled loss	0 – 200	~1 W/m	100%
Controlled loss:			
Charge selector	12 – 20	42 kW	100%
Charge stripper	12 – 20	~1 kW	100%
Collimators	0 – 200	~1 kW	100%
Dump FS1-a	12 – 20	42 kW	0.03%
Dump FS1-b	12 – 20	12 kW	5%
Dump FS2	15 – 160	300 kW	0.03%
Dump BDS	150 – 300	400 kW	0.03%

Space Charge, Coupling Impedance, Instability

Space charge and other coupling impedances can have performance-limiting effects for machines of low energy, high peak intensity beams. In linacs beam halo can be generated through core-halo parametric resonances and resonances between the transverse and longitudinal motion [58 – 61] (Fig. 10). In rings it is necessary to avoid resonances excited by lattice nonlinearity in the presence of space charge induced tune spread [5]. Instability suppression in rings includes impedance reduction of major sources (e.g. extraction kicker [62] and resistive wall [63] impedances), tune and chromaticity manipulation, and feedback systems [64].

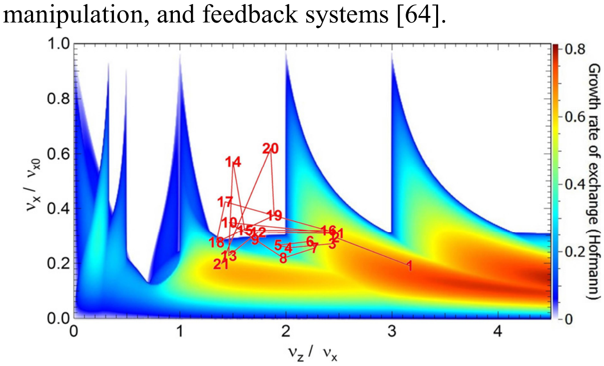

Figure 10: Tune footprint along the four IFMIF cryomodules superimposed to the Hofmann chart [60].

Multiple Charge State Acceleration

To reach high design beam intensity, simultaneous acceleration of heavy ion beams of multiple charge state is often needed due to the broad charge spectrum upon stripping. The FRIB driver linac accelerates up to five charge states simultaneously, transversely overlapping at charge stripper location and at the target (Fig. 11). Machine optics, diagnostics, and fault mitigation are designed in detail to meet the performance goals.

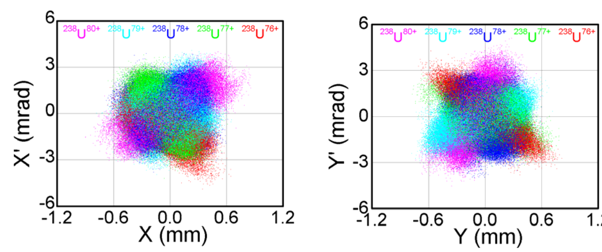

Figure 11: Five charge states of the uranium beam designed to overlap at the FRIB target.

Electron Cloud

Electron cloud limited the performance of the PSR proton accumulator at LANL [65]. Preventive measures were effective in the SNS ring suppressing electron generation and enhancing Landau damping [5] (Fig. 12).

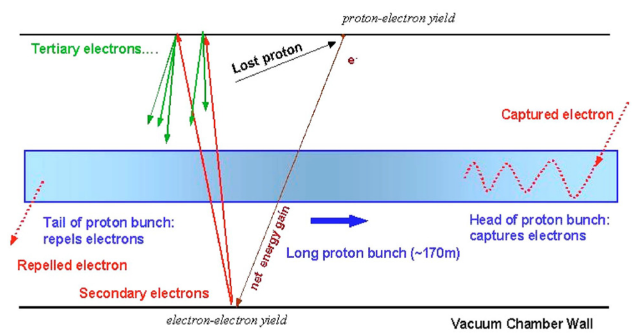

Figure 12: Beam-induced electron multipacting at the trailing edge of a long proton bunch [6].

Other topics include magnet interference [66] and fringe field [67] pertaining to large aperture and tight spacing, and H^- stripping issues [68 - 70].

FUTURE PERSPECTIVES

At a time when accelerator projects at the high-energy frontier are experiencing difficulties in gaining financial support, projects at the high-intensity frontier are flourishing worldwide. Demands for such accelerators extend from science to applications, and for primary beams from proton to heavy ions. Efforts worldwide are readying the technologies and designs meeting the requirements of user facilities with high reliability, availability, maintainability, tunability, and upgradability. With the present technology, we speculate to reach multi MW beam power using cyclotrons, synchrotrons or accumulators, and up to 100 MW with SRF linacs [71].

ISBN: 978-3-95450-132-8 doi:10.18429/JACoW-IPAC2014-MOYBA01

ACKNOWLEDGMENT

I thank D. Berkovits, Y.S. Cho, J. Erickson, R. Ferdinand, S. Fu, J. Galambos, R. Garoby, V. Ganni, R. Garnett, F. Gerigk, E. Gschwendtner, S. Henderson, S. Holmes, K. Jones, O. Kamigaito, O. Kester, J. Knaster, T. Koseki, M. Lindroos, P. Nghiem, K. Oide, S. Ozaki, M. Plum, T. Roser, M. Seidel, A. Taylor, J. Thomason, D. Vandeplassche, H. Zhao, F. Zimmermann for information and advice, G. Bollen, A. Facco, F. Marti, E. Pozdeyev, Y. Yamazaki and other FRIB colleagues for discussions.

REFERENCES

[1] N. Holtkamp, EPAC'02, 164 (2002); S. Henderson, LINAC'10, 11 (2010); J. Galambos, PAC'13, 1443 (2013).
[2] Y. Yamazaki, PAC'09, 18 (2009); K. Hasegawa et al, IPAC'13, 3830 (2013).
[3] M. Seidel et al, IPAC'10, 1309 (2010); P.A. Schmelzbach et al, HB'06, 274 (2006).
[4] D.E. Nagle, LINAC'72, 4 (1972); R.W. Garnett et al, PAC'11, 2107 (2011).
[5] J. Wei, Rev. Mod. Phys. 75, 1383 (2003).
[6] J. Wei et al, NA-PAC'13, 1453 (2013).
[7] T. Roser, PAC'01, 714 (2001).
[8] The CNGS Conceptual Technical Design, ed. K. Elsener, CERN Report CERN 98-02 (1998)
[9] M. Martens et al, PAC'07, 1712 (2007)
[10] PIP-II Whitepaper, FNAL Report: http://projectx-docdb.fnal.gov/cgi-bin/ShowDocument?docid=1232
[11] O. Kamigaito et al, IPAC'13, 333 (2013).
[12] R. Ferdinand et al, IPAC'13, 3755 (2013).
[13] O. Kester, IPAC'13, 1085 (2013).
[14] D. Findlay, PAC 695 (2007); J. Thomason et al, IPAC'13, 2678 (2013)
[15] D. Berkovits et al, LINAC'12, 100 (2012).
[16] S. Fu et al, IPAC'13, 3995 (2013).
[17] M. Lindroos et al, LINAC'12, 768 (2012).
[18] B. Choi et al, APAC'04, 231 (2004); Y. Cho et al, IPAC'13, 2052 (2013).
[19] J. Knaster et al, Nucl. Fusion 53, 116001 (2013).
[20] W. Zhan, IPAC'13, MOXAB101 (2013).
[21] D. Vandeplassche et al, IPAC'11, 2718 (2011).
[22] H.V. Smith Jr., et al, PAC'01, 3296 (2001).
[23] G.P. Lawrence et al, PAC'85, 2662 (1985).
[24] J. Yang et al, Nucl. Instrum. Meth. B 317, 263 (2013).
[25] D. Jeon, IPAC'13, 3898 (2013).
[26] X. Guan et al, HIAT'13, 112 (2012).
[27] R. Garoby et al, J. Phys. 408, 012016 (2013); W. Bonivento et al, CERN Report CERN-SPSC-2013-024 / SPSC-EOI-010 (2013).
[28] C. Plostinar et al, LINAC'12, 924 (2012).
[29] T.P. Wangler et al, SRF'99, (336 (1999); Y. Cho, SRF'01, 95 (2001); S. Kim et al, APAC'04, 30 (2004).
[30] S. Simrock, SRF'03, 254 (2003); W. Schappert et al, SRF'11, 940 (2011); A. Neumann et al, Phys. Rev. ST-AB 13, 082001 (2010).
[31] J. Sekutowicz, LINAC'06, 506 (2006).
[32] A. Facco et al, IPAC'12, 61 (2012).
[33] V. Ganni et al, CEC-ICMC 59, 323 (2013).
[34] Z. Liu et al, IPAC'12, 969 (2012).
[35] J. Benitez et al, ECRIS'12, THXO02 (2012); C. Lyneis et al, Rev. Sci. Instrum. 79, 02A321 (2013).
[36] M.P. Stockli et al, Rev. Sci. Instrum. 85, 265 (2013).
[37] L. Young et al, LINAC'00, 336 (2000).
[38] P. Ostroumov et al, Phys. Rev. ST-AB 15, 110101 (2012).
[39] H. Imao et al, IPAC'13, 3851 (2013).
[40] A. Hershcovitch, J. Appl. Phys. 79, 5283 (1995).
[41] J. Nolen et al, FRIB Report FRIB-T30705-TD-000450 (2013).
[42] I. Yamane, Phys. Rev. ST-AB 1, 053501 (1998); V. Danilov et al, Phys. Rev. ST-AB 10, 053501 (2007).
[43] A. Facco et al, Phys. Rev. ST-AB 10, 091001 (2007).
[44] H. Ludewig et al, PAC'99, 548 (1999); N. Catalan-Lasheras et al, Phys. Rev. ST-AB 4, 010101 (2001).
[45] F. Pellemoine, Nucl. Instrum. Meth. B317, 369 (2013).
[46] D.M. Jenkins, ICANS XIX (2010).
[47] B. Riemer et al, AccApp'13, THZTA02 (2013).
[48] S. Halfon et al, Rev. Sci. Instrum. 85, 056105 (2014).
[49] H. Aït Abderrahim, AccApp'11, 1 (2011).
[50] J. Wei, EPAC'04, 156 (2004); G.R. Murdoch et al, EPAC'06, 1831 (2006).
[51] R. Gupta et al., IEEE Trans. Appl. Superconduct. 21, 1888 (2011).
[52] C. Gardner et al, EPAC'94, 979 (1994).
[53] G.T. Danby et al, PAC'89, 384 (1989).
[54] C.M. Warsop, AIP Conf. Proc. 448, 104 (1998).
[55] B. Boardman, Ed., RAL Report RL 82-006 (1982).
[56] M. Kinsho, EPAC'08, 2897 (2008).
[57] R. Ronningen et al, FRIB Report FRIB-Z00000-TR-000025 (2010).
[58] I. Hofmann, et al, PAC'01, 2902 (2001).
[59] A. Fedotov et al, Phys. Rev. ST-AB 5, 024202 (2002).
[60] P.A.P. Nghiem et al, Laser Part. Beams 32, 109 (2014).
[61] F. Scantamburlo et al, these proceedings
[62] D. Davino et al, EPAC'02, 1467 (2002).
[63] Y.H. Chin et al., HB'08, 40 (2008).
[64] O. Konstantinova et al, IPAC'13, 1739 (2013).
[65] R. Macek et al, PAC'01, 688 (2001).
[66] Y. Papaphilippou et al, PAC'01, 1667 (2001).
[67] J. Wei et al, Part. Accel. 55, 339 (1996); Y. Papaphilippou et al, Phys. Rev. E 67, 046502 (2003).
[68] G.M. Stinson et al, Nucl. Instrum. Meth. 74, 333 (1969); A. J. Jason et al, LANL Report LA-UR-81-1257 (1981).
[69] H.C. Bryant et al, J. Mod. Optics 53, 45 (2006).
[70] V. Lebedev et al, LINAC'10, 929 (2010).
[71] For example, it is feasible to design a CW superconducting RF linac accelerating proton beams of 20 mA to 10 GeV. Challenges include technical aspects discussed in this paper as well as the cost, reliability and efficiency. Depending on the application, target technology demands separate developments.